Journal of Radioanalytical and Nuclear Chemistry, Vol. 248, No. 2 (2001) 309–313

Digital signal processing and zero-dead-time counting

M. Blaauw,[1] R. F. Fleming,[2] R. Keyser[3]

[1] *Interfaculty Reactor Institute, Delft University of Technology, Mekelweg 15, 2629 JB Delft, The Netherlands*
[2] *University of Michigan, 2355 Bonisteel Blvd, Ann Arbor, MI 48109-2104, USA*
[3] *PerkinElmer Instruments, Inc. ORTEC, 801 South Illinois Avenue, Oak Ridge, TN 37831, USA*

(Received December 13, 2000)

One of the most recent developments in equipment for high and/or varying count rates, as encountered in the gamma-ray spectrometry needed for INAA via short-lived radionuclides, is the advent of EG&G Ortec's DSPEC$^{plus™}$. This all-in-one apparatus provides digital signal processing and zero-dead-time counting. One such DSPEC unit was tested at IRI with respect to performance as a function of count rate. Optimum parameter settings for different applications were established. It is concluded that this spectrometer allows for measurements with count rates up to at least 10^5 cps with an accuracy of a few percent (depending on the calibration approach), a peak position stability of $5 \cdot 10^{-3}$%. and a peak width stability of 5%. It is also concluded that the normal spectrum provides a good estimate for the uncertainties in the zero-dead-time spectrum acquired with this spectrometer.

Introduction

The problem of varying dead time is a well-known source of error in gamma-ray spectrometry.[1–3] Under such conditions, dead time corrections can only be accurate if the varying dead time is dominantly caused by the radionuclide that is to be measured: values for other radionuclides present in the same spectrum will suffer.

Solutions have been offered in several forms: dead-time stabilization,[4,5] e.g., solves the problem at the cost of a fixed, perhaps unnecessary dead time and resulting loss of counting efficiency. Sources moving according to activity relative to the detector have been proposed[6] but results have not been forthcoming for mixed radionuclide applications.

Loss-free counting was introduced before the advent of the digital spectrometer by WESTPHAL,[7] improving on HARMS' differential dead time correction method.[8] The loss-free spectrometer measures instantaneous dead time with a virtual pulser and adds a corresponding number of counts to the channel in the MCA determined by the pulse digitized at that time. It would be a fallacy to think that this method increases information throughput of the spectrometer, it only solves the problem of varying dead-time corrections. On the downside, it introduces non-Poisson statistics in the channel contents of the loss-free spectrum. Early on, it was proposed to acquire both the loss-free and the "normal" (i.e., uncorrected) spectrum, and determine the uncertainties in peak areas using the normal spectrum. Some commercially available software packages, such as Hypermet, can handle such dual spectra.[9]

The analog WESTPHAL unit was difficult to adjust, but several authors have reported positive experiences.[10,11]

The advent of digital spectrometry allowed for digital implementations of the loss-free principle. Canberra introduced a loss-free digital spectrometer in the late 90s, that was found to function properly if the decaying radionuclide emitted the higher-energy gamma-rays, but sometimes failed to perform within specifications if low energy gamma-rays were the cause of the dead time.[12]

In 1999, Ortec introduced the DSPEC$^{plus™}$, naming the loss-free counting method "zero dead-time counting". This name might again cause people to believe that actual spectrometer throughput is now unlimited, but this is not the case as was discussed above. The difference between zero-dead-time and loss-free counting lies in the method of determination of instantaneous dead time, which is based on the GEDCKE-HALE live-time clock.[13] Also, zero-dead-time corrections are performed entirely digitally in zero-dead-time counting.

In this paper, experiences with the DSPEC$^{plus™}$ are presented and results of experiments performed with low-energy gamma-rays causing dead time presented. All measurements were performed with constant count rates to allow for statistical testing of reproducibility.

DSPEC$^{plus™}$ shaping parameters

In Figure 1, the shaping parameters are illustrated that were controlled in the experiments performed in this work, and that determine the shape of the pulse offered to the ADC by the digital amplifier-equivalent. The rise-time and flattop time together are equivalent to the analog amplifier shaping time setting. The processing time required for a single pulse is given by $3 \times$ rise + flat, according to Ortec.

0236–5731/2001/USD 17.00

Akadémiai Kiadó, Budapest
Kluwer Academic Publishers, Dordrecht

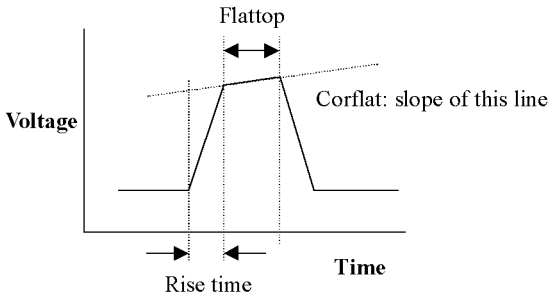

Fig. 1. Graphical representation of the shaping parameters

Experimental

Detector and counting geometry

The detector used was a HpGe detector with a relative efficiency of 40% and a FWHM at 1333 keV of 1.7 keV (manufacturer specifications) or 2.1 keV (measured with analog spectrometer) in a vertical dipstick geometry. A 2.5 kBq ^{137}Cs source was attached to the end cap of the detector at a distance of approx. 5 cm. A lead-encased 37 MBq ^{241}Am source, emitting an intense, narrow beam of 60 keV gamma-rays, was placed in various positions to introduce different dead times.

The detector was connected to the DSPEC$^{plus™}$ for a high voltage of 3.5 kV, preamp power and signal digitization.

Measurements

Varying shaping parameters: In the absence of the ^{241}Am source, spectra were acquired in 1200 seconds each of the ^{137}Cs source at 7 rise time settings (2, 4, 5, 6, 7, 8, and 10 μs), 6 flattop settings (0.3, 0.5, 1.0, 1.5, 2.0, 2.3 μs) and 7 "corflat" values (–1.0, –0.5, –0.25, 0.0, 0.25, 0.5, and 1.0) for a total of 294 spectra.

Varying dead time: After positioning of the ^{241}Am source to obtain a desired count rate, 20 measurements were performed in extended-live-time mode, with alternating shaping parameter settings, (risetime 2 μs, flattop 0.3 μs, corflat 0.5, and rise-time 4 μs, flattop 0.5 μs and corflat 0.0) followed by 20 measurements in zero-dead-time mode, with the same alternating shaping parameters settings.

Data handling

Shaping parameters optimization: A two-tailed Gaussian function was fitted to the 662 keV peak position in all 294 spectra obtained with varying shaping parameters to determine the peak shape and position of the 662 keV peak. From the resulting dataset, two combinations of parameters were selected: the threesome that resulted in the highest peak position channel, and the threesome that resulted in the smallest peak width at the lowest rise time of 2 μs. The two settings thus obtained were used in the controlled-dead time measurements.

Varying dead time: The 662 keV peak area count rates in all controlled-dead-time spectra were determined by integration and continuum subtraction, in order to maintain a firm grasp on the statistical aspects. To this end, firstly a two-tailed Gaussian function was fitted to each of the spectra (except the ZDT spectra) obtained at one count rate, to establish peak position and shape. Then, the region to be integrated (for the normal spectra as well as the ZDT spectra) was taken as the group of channels where the value of the two-tailed normalized Gaussian function exceeded 10^{-5}. The continuum under the peak was to be estimated as the average channel content in the regions to the left and right of the integrated region, each with a width of two standard deviations of the Gaussian. The regions to be employed for all 10 spectra obtained at one count rate and shaping-parameters setting were then determined by averaging the values found for the individual spectra. The formula employed was:

$$A = \sum_{i=b}^{c} p_i - \frac{(c-b+1)}{(b-a)+(d-c)}\left(\sum_{i=a}^{b-1} p_i + \sum_{i=c+1}^{d} p_i\right)$$

where A is the peak area, p_i is the content of channel i, a and b delimit the left continuum region, b and c delimit the peak region and c and d delimit the right continuum region.

The internal 1 s.d. uncertainty of the peak area $\sigma_{int,A}$ was computed with:

$$\sigma^2_{\mathrm{int},A} = \sum_{i=b}^{c} p_i + \left(\frac{(c-b+1)}{(b-a)+(d-c)}\right)^2\left(\sum_{i=a}^{b-1} p_i + \sum_{i=c+1}^{d} p_i\right)$$

The external standard deviation of 10 peak areas was obtained by:

$$\sigma^2_{\mathrm{ext},A} = \sqrt{\frac{\sum_{i=1}^{10}(A_i - \langle A\rangle)^2}{N-1}}$$

where $<A>$ is the unweighted average of the 10 peak areas A_i. From the internal and external standard deviations, standard errors of the mean $\mathrm{SEM_{int}}$ and $\mathrm{SEM_{ext}}$ were obtained through division by $\sqrt{N}$, where N is the number of spectra.

From the peak areas and associated uncertainties, the peak area count rates were obtained through division by the live time reported by the DSPEC (which it does even in ZDT mode), except for the peak areas from the ZDT-corrected spectra, that were divided by the real time as reported by the DSPEC.

The 10 measurements in zero-dead time mode yielded 20 spectra (one corrected, one uncorrected) that were treated as two separate sets for analysis purposes.

Results

Varying shaping parameters

In Fig. 2, the typical shapes of the relations between peak width, position and rise-time are shown, measured at a flat top duration of 0.5 μs and a flat correction of 0.0. These results are comparable to those seen with analog systems.

Varying dead time

In Figs 3 and 4, the 662 keV peak area count rates are shown for resp. extended-live-time mode and zero-dead-time mode as a function of count rate. The dead-time plotted in the zero-dead-time graph was computed from the reported live and real time.

In Fig. 5, the stability of FWHM and peak position as a function of count rate are plotted from the fit results of the normal spectra obtained in ZDT-mode. The peak position varies with a relative standard deviation of $6 \cdot 10^{-3}$% at a 2 μs risetime, and $5 \cdot 10^{-3}$% at 5 μs. The FWHM increase slightly with count rate, with 2% at 2 μs and 5% at 5 μs (but the FWHM at 5 μs is smaller than the FWHM at 2 μs at all count rates).

In Fig. 6, the effectivity of the dual spectrum method to account for the distorted statistics in the ZDT spectrum is demonstrated. Plotted are the SEM_{ext}/SEM_{int} ratios, being the ratios of expected and observed variations, obtained in two ways: One SEM_{int} was determined from the channel contents of the ZDT spectrum and converted to the SEM of the count rate by division through real time, the other from the channel contents of the normal spectrum and division through live time as reported by the DSPEC^{plus}™.

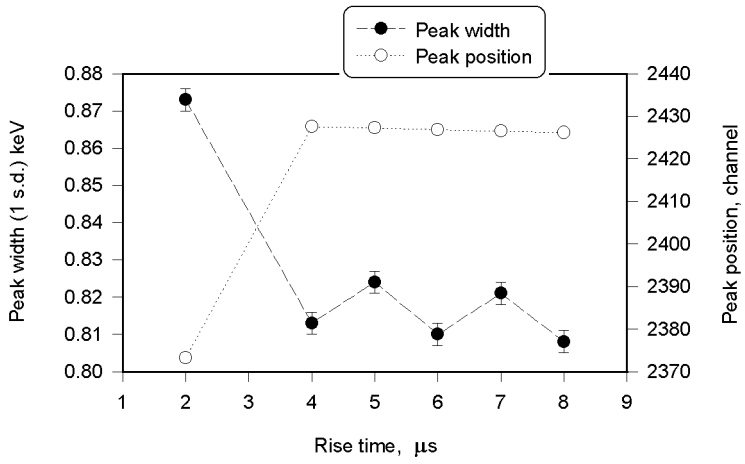

Fig. 2. Peak shape and position as a function of rise-time. Lines were drawn to guide the eye

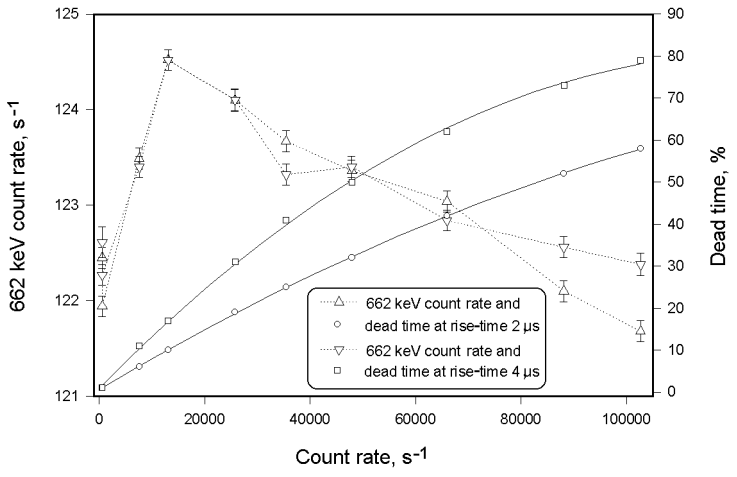

Fig. 3. Extended-live-time mode 662 keV peak area count rates and dead time as a function of count rate at two rise time settings. The uncertainties plotted are the SEM_{int}. Lines were drawn to guide the eye

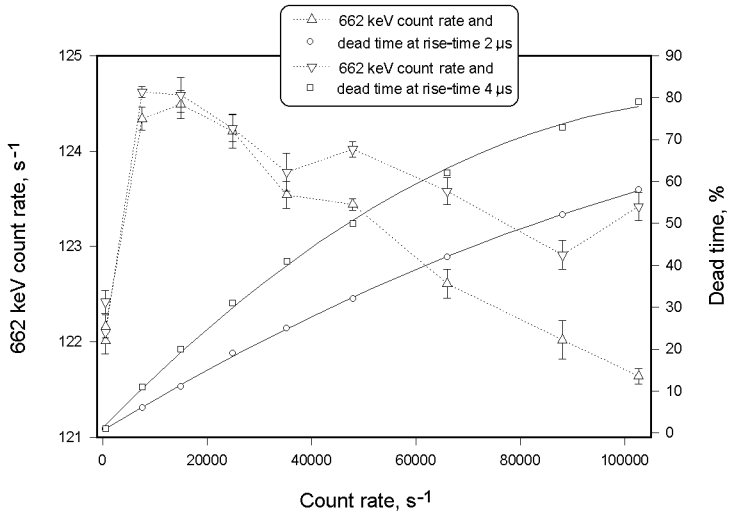

Fig. 4. Zero-dead-time mode 662 keV peak area count rates and "dead time" as a function of count rate at two rise-time settings. The uncertainties plotted are the SEM_{ext}. Lines were drawn to guide the eye

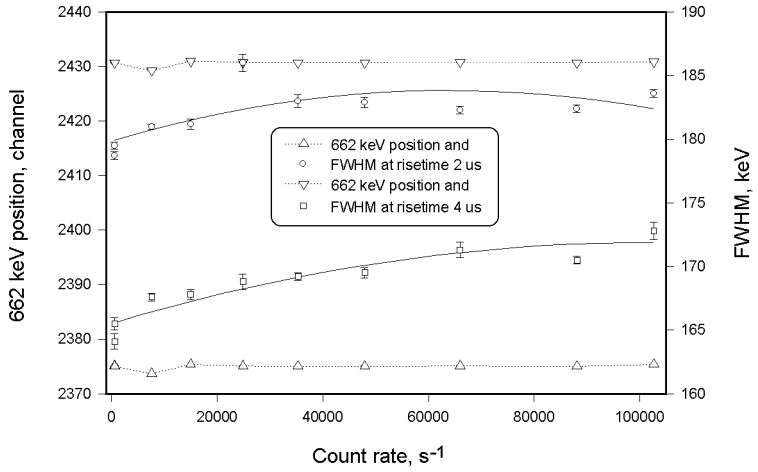

Fig. 5. Peak position and FWHM as a function of count rate. Lines were drawn to guide the eye

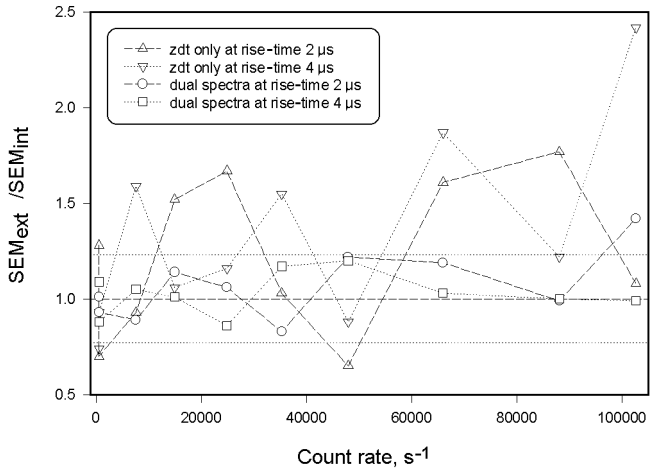

Fig. 6. SEM_{ext}/SEM_{int} ratios showing the effectivity of the dual spectrum method. The horizontal lines indicate the expected value and the 67% confidence interval for such ratios obtained from 10 determinations

Discussion

The DSPEC$^{plus™}$ stably corrects for dead-time in zero-dead-time mode. In the tested case of constant count rates, it performs as well in zero-dead-time mode as in extended-live-time mode. The variation in peak areas obtained is in the order of 1 to 2%, but is not random. The error made when determining radionuclide activities will depend on the difference in count rate between calibration and sample measurement. Only, if the calibration is performed at, say, $5 \cdot 10^4$ cps, the accuracy of all sample measurements will be 1% with respect to dead-time correction.

Remarkably, it is observed that the observed peak area count rates increase markedly as the count rate increases from 0 to 10^4 cps, and then decreases more slowly as the count rate increases to 10^5 cps. It seems risky to extrapolate the curve at higher count rates to 0 and call the intercept the "reference value", as POMMÉ and KENNEDY[14] did in their testing of the preceding DSPEC model. Apart from that, the results presented here are equivalent to those obtained by POMMÉ and KENNEDY.[14]

The peak position and FWHM are nicely stable in ZDT mode at both rise times employed. The FWHM at 2 μs are slightly worse than at 5 μs (1.8 vs. 1.7 keV), but stabler as a function of count rate. In practice, when dead time is expected to vary a great deal, one might, therefore, prefer the shorter rise time from the viewpoint of fittability of the peaks alone.

The peak area statistics are under control, i.e., observed and expected variations are equal, when the dual spectrum method is used. Without that, control clearly deteriorates with increasing count rate.

Conclusions

The DSPEC$^{plus™}$ stably corrects for dead time in zero-dead-time mode. The accuracy of all sample measurements will be 1% with respect to dead-time correction if the calibration is performed at elevated count rates of about $5 \cdot 10^4$ cps. The peak position is stable with a standard deviation of $5 \cdot 10^{-3}$%, the FWHM varies by 5% at 5 μs rise-time and by 2% at 2 μs rise-time.

The dual-spectrum solution for the distorted counting statistics yields good estimates for the uncertainties in the zero-dead-time corrected peak areas.

References

1. E. SCHÖNFELD, Nucl. Instr. Meth., 42 (1966) 213.
2. W. GÖRNER, G. HÖHNEL, Nucl. Instr. Meth., 88 (1970) 193.
3. M. WIERNIK, Nucl. Instr. Meth., 95 (1971) 13.
4. J. BARTOSEK, F. ADAMS, J. HOSTE, Nucl. Instr. Meth., 103 (1972) 45.
5. M. DE BRUIN, S. S. THEN, P. BODE, P. J. M. KORTHOVEN, Nucl. Instr. Meth., 121 (1974) 611.
6. N. N. PAPDOPOULOS, G. E. HATZAKIS, A. C. SALEVRIS, N. F. TSAGAS, J. Trace and Micropr. Techn., 14 (1996) 1.
7. G. P. WESTPHAL, Nucl. Instr. Meth., 163 (1979) 189.
8. J. HARMS, Nucl. Instr. Meth., 53 (1967) 192.
9. B. FAZEKAS, T. BELGYA, L. DABOLCZI, G. MOLNÁR, A. SIMONITS, J. Trace Micropr. Techn., 14 (1996) 167.
10. R. M. LINDSTROM, M. J. J. AMMERLAAN, S. S. THEN, J. Trace Micropr. Techn., 14 (1996) 67.
11. S. R. BIEGALSKI, S. LANDSBERGER, K. HEYDORN, J. Trace Micropr. Techn., 14 (1996) 87.
12. A. SIMONITS, J. Radioanal. Nucl. Chem., Proc. of the MTAA-10 Conference, in press.
13. R. JENKINS, R. W. GOULD, D. GEDCKE, Quantitative X-ray Spectrometry, Marcel Dekker, New York, 1981.
14. S. POMMÉ, G. KENNEDY, Appl. Radiation Isotopes, 52 (2000) 377.